Demodulation of Polarimetric Fibre Laser Ultrasonic Sensor with Intensity Noise Cancellation

Jianfei Wang, Gordon M. H Flockhart*, Deepak Uttamchandani

***Abstract*—In this paper, the influences of the relative intensity noise (RIN), in particular the relaxation oscillation noise, of an erbium distributed feedback (DFB) fibre laser has been investigated theoretically and experimentally for use a polarimetric ultrasonic sensor. We show that the relaxation oscillation noise and the ultrasonic signal both induce modulation sidebands on the polarization beat frequency of the DFB laser ultrasonic sensor. We present a novel demodulation algorithm for the polarimetric DFB fibre laser ultrasonic sensor, which can effectively eliminate the influences of the intensity noise and slowly varying drift of the polarization beat frequency.**

***Index Terms* — ultrasonic sensor; fibre laser; intensity noise**

I. Introduction

OPTICAL fibre lasers based on fibre Bragg grating structures have been investigated for high-performance optical sensing applications due to their narrow frequency linewidth and noise properties [1], [2]. To achieve high-sensitivity sensors, small changes in the laser frequency are measured, typically using path imbalanced interferometers. Polarimetric optical fibre Bragg grating (FBG) laser sensors obviate the need for large path imbalanced interferometers by heterodyning two orthogonal polarization lasing modes, with slightly different lasing frequencies, to produce a lower frequency polarization beat frequency [3], [4]. This work utilized distributed feedback (DFB) structures which contain a π-phase-shifted FBG; however single-longitudinal mode and single-polarization mode distributed Bragg reflector (DBR) structure were also demonstrated [5]. Recently heterodyning DBR fibre grating laser sensors, with outstanding characteristics of high sensitivity, compact size and broad bandwidth, have been investigated for a range of measurands and applications [6]. In particular, acoustic and ultrasonic fibre laser sensors have attracted considerable interest due to promising applications in biomedical photoacoustic imaging [7]–[13]. The laser's polarization beat frequency changes when the laser cavity is subjected to an ultrasonic acoustic field, owing to the variation of the fiber birefringence. The response of the polarimetric heterodyning ultrasonic laser sensor does not depend on whether the laser has a DBR or a DFB structure, but the frequency response depends on the composition and geometry of the optical fibre and coating [14]. The key requirement for the laser sensor is controlled fabrication of grating structures allowing dual-polarization stable single-longitudinal mode lasing output.

Fundamental characteristics of the polarimetric heterodyning fibre grating laser ultrasonic sensor, such as sensitivity, linear responses, bandwidth and so on, have been studied previously [7] – [13]. Intensity and frequency noise in fibre laser structures has been extensively investigated [2], [15]–[19]. The relaxation oscillation contributes to a noise peak in both the relative intensity noise (RIN) and the frequency noise of the fibre grating laser. Depending on the amplitude and frequency of this noise peak, the performance of the laser sensor can be adversely affected. The influence of the relaxation oscillation noise on polarimetric fibre laser sensors has not been investigated previously. Prior work has demonstrated the polarization beat frequency spectrum for both DFB [20] and DBR fibre lasers [6] [7], [21]–[23]; however, this does not show any influence of noise on the polarization beat frequency from the relaxation oscillation.

In this paper, the influences of the RIN on the performance of a polarimetric fibre laser ultrasonic sensor based on a DFB grating structure have been investigated theoretically and experimentally. We observe modulation sidebands on the polarization beat frequency and a novel demodulation algorithm of the DFB fibre ultrasonic sensor that eliminates the influence of the noise is presented. The result could also be applied in the DBR fiber laser based polarimetric heterodyning ultrasonic sensor.

II. Theory

A. Sensing principle

Figure. 1 shows the configuration of the DFB fibre laser. It consists of a periodic refractive index grating (written directly

Manuscript received January 15, 2019.

This work was supported in part by the National Key R&D Program of China under Grant No 2017YFB0405500 and the National Natural Science Foundation of China under Grant No. 61705263.

Jianfei Wang is with the College of Meteorology & Oceanology, National University of Defense Technology, Changsha, 410073, China (e-mail: wjfjoy@126.com).

Gordon M. H. Flockhart is with the Centre for Microsystems & Photonics, Department of Electronic & Electrical Engineering, University of Strathclyde, Glasgow, G1 1XW, UK (e-mail:gordon.flockhart@strath.ac.uk).

Deepak Uttamchandani is with the Centre for Microsystems & Photonics, Department of Electronic & Electrical Engineering, University of Strathclyde, Glasgow, G1 1XW, UK (e-mail:d.uttamchandani@strath.ac.uk).

into a rare earth doped fibre) with a π-phase-shift in the center. The DFB fibre laser can offer stable single longitudinal lasing mode operation without mode hopping in principle. Typically, two orthogonal polarization modes lase within a DFB fibre laser due to the intrinsic and UV induced birefringence of the fibre. The wavelengths of the two orthogonal polarization modes of a DFB fibre laser can be expressed by

$$\lambda_{x,y} = 2n_{x,y}\Lambda \tag{1}$$

where $\lambda_{x,y}$ are the wavelengths of the two orthogonal polarization modes, $n_{x,y}$ are the effective refractive indices of the fibre, and Λ is the grating pitch. Consequently, a polarization beat signal can be observed when the two orthogonal polarization modes are optically mixed. For a low birefringent fibre with $n_x \approx n_y \approx n$ the beat frequency is given by

$$\Delta\nu = cB/\left(2n^2\Lambda\right) \tag{2}$$

where $B = |n_x - n_y|$ is the birefringence and c is the velocity of light in vacuum.

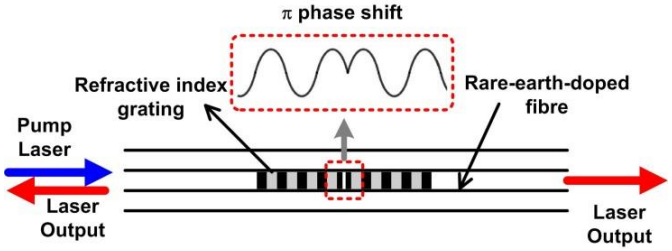

Fig. 1. Schematic of the DFB fibre Laser Structure.

The general sensing principle has been reported previously [7]. When the DFB fibre laser is subjected into an ultrasonic acoustic field, the ultrasonic acoustic pressure modulates the fibre birefringence due to the different refractive index changes along and perpendicular to the propagation direction of the ultrasonic wave, and consequently the beat frequency of the two orthogonal polarization modes changes. The induced change in birefringence of the fibre can be expressed by [24]

$$\Delta B = kp\cos\left(\omega t\right)\cos\left(2\theta\right) \tag{3}$$

where k is a coefficient depending on the ultrasonic frequency, the photo-elastic coefficient and refractive index of the fibre. p and ω are the amplitude and angular frequency of the acoustic pressure, respectively. θ is the angle between the polarization axis of the fibre and the propagation direction of the ultrasonic wave.

The DFB fibre laser has a typical length of 3-5 cm [10]. However, the DFB fibre laser mode profile is Lorentzian centered about the π-phase-shift; thus the effective sensitive region is about 5-10 mm [11]. Therefore, we must consider a position coefficient $I(x)$ in Eq. (3), which depends on the laser mode intensity distribution along the laser. Furthermore, the ultrasonic pressure p along the laser is also not uniform. Assuming the DFB fibre laser is parallel to the acoustic wave front, the induced beat frequency change is given by

$$\delta\Delta\nu = \Delta\nu\frac{k\int_0^L I\left(x\right)pdx}{BL}\cos\omega t\cos 2\theta \tag{4}$$

Where L is the length of the DFB fibre laser. Therefore, the output of the DFB sensor is the line integral of the laser intensity as well as the ultrasonic pressure amplitude along the laser.

B. Beat signal

The two orthogonal polarization modes of the DFB fibre laser can be expressed by

$$E_{x,y} = A_{x,y}\cos\left(\omega_{x,y}t + \varphi_{x,y}\right) \tag{5}$$

where $A_{x,y}$ $\omega_{x,y}$ and $\varphi_{x,y}$ are the amplitude, angular frequency and phase of the two orthogonal polarization modes, respectively. Then the intensity I of the corresponding beat frequency received by the high speed photodetector can be expressed as

$$I = \left(E_x + E_y\right)^2 = A^2\left(1 + \cos\left(\Delta\omega t + \Delta\varphi\right)\right) \tag{6}$$

where $A=A_x \approx A_y$, $\Delta\omega$ and $\Delta\varphi$ are respectively the beat angular frequency and the phase difference of the two orthogonal polarization modes, and the latter of which ($\Delta\varphi$) can be treated as constant. Through the analysis above, we understand that the ultrasound induces a frequency modulation (FM) of the beat frequency. Therefore, the output intensity of the DFB fibre laser ultrasonic sensor, which is subjected to an acoustic field, can be given as

$$I = A^2\left(1 + \cos\left(\Delta\omega t + K_F\int m\left(t\right)dt + \Delta\varphi\right)\right) \tag{7}$$

where $m(t)$ is the ultrasonic modulation signal, $K_F = \Delta\nu\frac{k\int_0^L I\left(x\right)dx}{BL}\cos 2\theta$ is defined as the frequency modulation sensitivity. It should be noted that, K_F can also be treated as the total sensitivity, although the sensitivity of DFB fibre laser sensor varies along the laser cavity.

Assuming the input ultrasonic signal is of a simple sinusoidal form,

$$m\left(t\right) = C\cos\omega_s t \tag{8}$$

where C and ω_s are the amplitude and angular frequency of the ultrasonic signal applied to the sensor. As a note, the acoustic pressure along the fibre laser is not uniform in most practical situations. We treat it as a constant here in order to

simplify the analysis. Substituting Eq. (8) into Eq. (7), the output of the DFB laser can be written as

$$I = A^2 \cos\left(\Delta\omega t + m_f \sin\omega_s t\right) = Re\left(A^2 e^{j\Delta\omega t} e^{jm_f \sin\omega_s t}\right) \quad (9)$$

$$m_f = CK_F / \omega_s \quad (10)$$

where m_f is defined as the FM index. For simplicity, we ignore the DC term A^2 and the phase term $\Delta\varphi$ in Eq. (9). Expending $e^{jm_f \sin\omega_s t}$ using Bessel functions, the Eq. (9) can be rewritten as

$$\begin{aligned} I &= \mathrm{Re}\left(A^2 e^{j\Delta\omega t} \sum_{n=-\infty}^{\infty} J_n(m_f) e^{jn\omega_s t}\right) \\ &= A^2 \sum_{n=-\infty}^{\infty} J_n(m_f) \cos(\Delta\omega + n\omega_s)t \\ &= A^2\{J_0(m_f)\cos\Delta\omega t + J_1(m_f)\cos(\Delta\omega + \omega_s)t - \\ &\quad J_1(m_f)\cos(\Delta\omega - \omega_s)t + J_2(m_f)\cos(\Delta\omega + 2\omega_s)t - \\ &\quad J_2(m_f)\cos(\Delta\omega - 2\omega_s)t + \cdots\} \end{aligned} \quad (11)$$

where $J_n(m_f)$ is a Bessel function of the first kind with argument, n is an integer.

Eq. (11) indicates that the output of the DFB fibre laser contains beat frequency and infinite pairs of sidebands. The frequency spacing of each adjacent frequency component is ω_s, which is the angular frequency of the ultrasonic signal. Therefore, the frequency of the ultrasonic signal could be determined by measuring the frequency shift of the upper or lower sidebands of the beat signal with a high speed photodetector and RF spectrum analyzer. The amplitudes of the beat frequency and sidebands are determined by the corresponding value of Bessel function, which varies with the change of m_f.

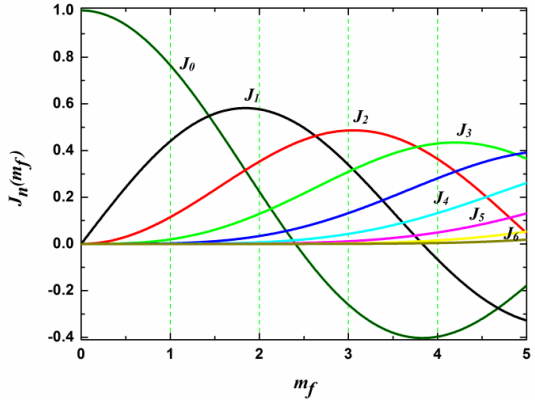

Fig. 2 Bessel functions of the first order versus m_f.

Figure. 2 shows the curves of the n-order Bessel functions of the first kind as a function of m_f. In consideration of m_f, it is reasonable to consider m_f as only determined by the amplitude of the applied ultrasonic signal C, because the sensitivity of the DFB fibre laser and the frequency of ultrasonic signal are fixed in practical applications. Through a comparative analysis between Eq. (10) and Fig. 2, it is evident that, more and more high order sidebands appeared as the amplitude of the ultrasonic signal increase, as evident in previous work [7].

We should also notice that, the amplitude of the ultrasonic signal cannot be determined simply by measuring the amplitude of the first-order sidebands of the beat signal, as the amplitudes of the sidebands do not show a linear dependence with the ultrasonic signal amplitude. Fortunately, when the value of m_f is small, the curve of the first-order Bessel function can be approximated as linear. Figure. 3 shows the first-order Bessel function and a linear fit (m_f <0.1). The numerical deviation of the two curves is larger than 5% when the value of m_f exceeds 0.6. Therefore, the amplitude of first-order sidebands can be used to determine the amplitude of the ultrasonic signal only when the value of m_f is smaller than 0.6. Assuming the sensitivity of the DFB fibre laser ultrasonic sensor is 1 kHz/Pa. If the frequency of signal is 10 MHz, the amplitude of first-order sidebands changes linearly only when the amplitude of signal is smaller than 6000 Pa. If the frequency of signal is 100 kHz, the amplitude of first-order sidebands changes linearly only when the amplitude of signal is smaller than 60 Pa.

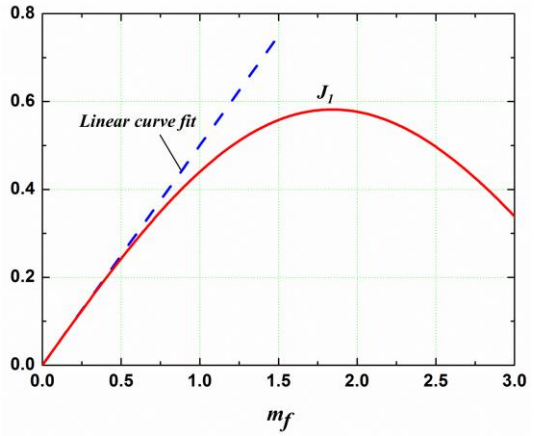

Fig. 3 The primal first-order Bessel function and a linear fit m_f <0.1.

C. *Effects of the fibre laser intensity noise*

The influences of RIN, in particular the relaxation oscillation noise, on the DFB fibre laser ultrasonic sensor must be considered in some practical applications.

The relaxation oscillation noise can potentially affect the polarization beat frequency through two mechanisms. The relaxation oscillation gives rise to an in-phase intensity modulation on each orthogonal polarization mode. This intensity modulation gives rise to a sum and difference frequency shift of the polarization beat frequency through heterodyning the two modes and has been observed in a Nd:YAG microchip laser [25]. A second mechanism is through direct frequency modulation of the laser modes due to small perturbations of the mode's effective refractive indices. The relaxation oscillation leads to intensity variation due to changes in gain and pump absorption, which comes from changes in the energy level populations of the gain medium [15]. This results in small perturbations of the optical fibre's temperature due to self-heating and a corresponding change in refractive index through the thermo-optic effect. In addition, changes in

absorption modify the refractive index through the Kramers-Kronig relations. However, in our consideration the magnitude of this is negligible compared to the other effects.

Based on the analysis of the Nd:YAG microchip laser [25], we treated the intensity noise of the DFB fibre laser as a single frequency signal. The total intensity noise can be treated as the superposition of multiple single noise signals. The two orthogonal polarization modes of the DFB fibre laser can by expressed by

$$E_{x,y} = A\left(1 + k_n \cos\omega_n t\right)\cos\left(\omega_{x,y} t + \varphi_{x,y}\right) \tag{12}$$

where k_n ($k_n << 1$) and ω_s are amplitude and angular frequency of the intensity noise signal. Inserting Eq. (12) into Eq. (6), the intensity of the beat signal received by photodetector can be rewritten as

$$\begin{aligned} I \approx\ & A^2\left\{1 + 2k_n \cos\omega_n + \cos\left(\Delta\omega t + \Delta\varphi\right)\right. \\ & + k_n \cos\left[\left(\Delta\omega + \omega_n\right)t + \Delta\varphi\right] \\ & \left. + k_n \cos\left[\left(\Delta\omega - \omega_n\right)t + \Delta\varphi\right]\right\} \end{aligned} \tag{13}$$

where we have ignored the high frequency parts of $2\omega_x$, $2\omega_y$ and $\omega_x+\omega_y$, and the higher order terms of k_n are also neglected.

Equation. (13) indicates that, the beat signal of the two orthogonal polarization modes includes four frequency components: intensity noise frequency (ω_n), beat frequency ($\Delta\omega$) and a pair of sidebands of the beat frequency ($\Delta\omega+\omega_n$, $\Delta\omega-\omega_n$). It should be noted that the pair of sidebands is caused by intensity noise rather than ultrasonic signals.

The output of the DFB laser including the ultrasonic signal and the laser intensity noise can be obtained by inserting Eq. (12) into Eq. (9).

$$I = I_1 + I_2 \tag{14}$$

$$I_1 = A^2 \sum_{n=-\infty}^{\infty} J_n\left(m_f\right)\cos\left(\Delta\omega + n\omega_s\right)t$$

$$= A^2 \begin{bmatrix} J_0\left(m_f\right)\cos\Delta\omega t + J_1\left(m_f\right)\cos\left(\Delta\omega + \omega_s\right)t \\ -J_1\left(m_f\right)\cos\left(\Delta\omega - \omega_s\right)t + \\ J_2\left(m_f\right)\cos\left(\Delta\omega + 2\omega_s\right)t - \\ J_2\left(m_f\right)\cos\left(\Delta\omega - 2\omega_s\right)t + \cdots \end{bmatrix} \tag{15}$$

The expression of Eq. (15) as well as the physical explanation of I_1 is the same with Eq. (11). It indicates that the DFB fibre laser output contains beat frequency and infinite pairs of sidebands. The frequency spacing of each adjacent frequency component is ω_s. The amplitudes of the beat frequency and sidebands are determined by the corresponding value of Bessel function, which varies with the change of m_f.

$$I_2 = 2k_n A^2 \sum_{n=-\infty}^{\infty} J_n\left(m_f\right)\cos\omega_n t \cdot \cos\left(\Delta\omega + n\omega_s\right)t$$

$$= k_n \mathrm{A}^2 \begin{bmatrix} J_0\left(m_f\right)\cos\left(\Delta\omega + \omega_n\right)t + \\ J_0\left(m_f\right)\cos\left(\Delta\omega - \omega_n\right)t \\ +J_1\left(m_f\right)\cos\left(\Delta\omega + \omega_s + \omega_n\right)t + \\ J_1\left(m_f\right)\cos\left(\Delta\omega + \omega_s - \omega_n\right)t - \\ J_1\left(m_f\right)\cos\left(\Delta\omega - \omega_s + \omega_n\right)t \\ -J_1\left(m_f\right)\cos\left(\Delta\omega - \omega_s - \omega_n\right)t + \cdots \end{bmatrix} \tag{16}$$

Equation. (16), the expression of I_2 indicates that the intensity noise signal will induce sidebands of each frequency component of I_1. And the amplitudes of these sidebands are determined by the products of k_n, A^2 and the corresponding value of Bessel function $J_n(m_f)$. In most cases, these sidebands cannot be observed because $k_n<<1$ and the value of the corresponding Bessel functions is also small. However, it cannot be ignored with the increasing of $J_n(m_f)$.

III. Demodulation Algorithm

The above analysis concludes that the ultrasonic signal cannot be simply determined by measuring the frequency shift and the amplitude of the sidebands to the beat signal. The intensity noise of the DFB fibre laser will also induce sidebands of the beat signal. In some practical applications, we wish to record the in situ time domain waveforms of the ultrasonic signals. Therefore, it is necessary to investigate demodulation methods for the ultrasonic sensor based on the DFB fibre laser.

The arc-tangent algorithm, which is also called the I/Q quadrature algorithm, has been used to demodulate ultrasonic signals in DBR fibre laser sensor systems [11], [12]. The flow diagram of the arc-tangent demodulation algorithm is shown in Fig. 4. The frequency modulated signal is mixed with two low noise quadrature local carriers.

The two local carriers have an identical frequency very close to that of the beat frequency and have a 90-degree phase offset. After this quadrature down conversion, two baseband signals $I(t)$ (In-phase) and $Q(t)$ (quadrature) are used to depict the modulated signal. The phase information can be extracted via $\phi(t) = \arctan(Q(t)/I(t))$. The frequency variation of the beat signal can be subsequently recovered by taking the derivative of the phase data.

Theoretically, in order to get the modulated signal without distortion, the frequency of the local carrier and the beat frequency must be strictly equal. However, a stable beat frequency of the fibre laser is difficult to achieve in practical applications. Small environmental perturbations, especially from temperature, will cause the laser beat frequency to drift. Therefore, the arc-tangent algorithm is unsuitable for practical fibre laser sensor systems unless we can implement real-time feedback of the beat signal frequency to the demodulation system. For a high frequency beat signal (several hundred MHz to GHz), it is unrealistic to instantaneously measure the

frequency with high accuracy.

Therefore, we propose a novel demodulation algorithm, which can effectively eliminate the influences of the beat frequency shift and the unwanted influence of the relaxation oscillation noise.

A. *Improved I/Q Quadrature Demodulation Algorithm*

Through the theoretical analysis, we understand that the sensing principle of the DFB fibre laser ultrasonic sensor is based on the ultrasound induced FM of the fibre laser beat frequency. Considering the intensity noise of the DFB fibre laser, Eq. (7) can be expressed as

$$S(t) = a(t)\left(1 + \cos\left(\Delta\omega t + K_F\int m(t)\,dt + \Delta\varphi\right)\right) \quad (17)$$

where $a(t)$ is the amplitude of the sensor output by considering the intensity noise of the DFB fibre laser. Multiplying Eq. (17) with two low noise quadrature local carriers $\cos(\Delta\omega t)$ and $\sin(\Delta\omega t)$.

$$S_I(t) = S(t)\cos(\Delta\omega t) = a(t)\cos(\Delta\omega t) + \frac{1}{2}a(t)\left\{\cos\left[2\Delta\omega t + K_F\int m(t)\,dt + \Delta\varphi\right] + \cos\left[K_F\int m(t)\,dt + \Delta\varphi\right]\right\} \quad (18)$$

$$S_Q(t) = S(t)\sin(\Delta\omega t) = a(t)\sin(\Delta\omega t) + \frac{1}{2}a(t)\left\{\sin\left[2\Delta\omega t + K_F\int m(t)\,dt + \Delta\varphi\right] - \sin\left[K_F\int m(t)\,dt + \Delta\varphi\right]\right\} \quad (19)$$

Where the two local carriers have an identical frequency with the beating signal of DFB fibre laser sensor and have a 90-degree phase offset. Passing $S_I(t)$ and $S_Q(t)$ through low-pass filters, we get the following equations

$$I(t) = \frac{1}{2}a(t)\cos\left[K_F\int m(t)\,dt + \Delta\varphi\right] \quad (20)$$

$$Q(t) = \frac{1}{2}a(t)\sin\left[K_F\int m(t)\,dt + \Delta\varphi\right] \quad (21)$$

By taking the derivative of $I(t)$ and $Q(t)$, we have the following expressions

$$I'(t) = \frac{1}{2}\left\{a'(t)\cos\left[K_F\int m(t)\,dt + \Delta\varphi\right] - a(t)K_F m(t)\sin\left[K_F\int m(t)\,dt + \Delta\varphi\right]\right\} \quad (22)$$

$$Q'(t) = \frac{1}{2}\left\{a'(t)\sin\left[K_F\int m(t)\,dt + \Delta\varphi\right] + a(t)K_F m(t)\cos\left[K_F\int m(t)\,dt + \Delta\varphi\right]\right\} \quad (23)$$

Then we can get the ultrasonic signal which is detected by DFB fibre laser sensor by using the following formula.

$$M(t) = K_F m(t) = \frac{I(t)Q'(t) - I'(t)Q(t)}{I^2(t) + Q^2(t)} \quad (24)$$

Where $M(t)$ is the final signal detected by DFB fibre laser sensor, $m(t)$ is the applied ultrasonic signal, K_F is the sensitivity of the DFB fibre laser ultrasonic sensor.

It can be seen from the analysis above; the *I/Q* demodulation algorithm can eliminate the influence of the laser intensity noise completely in the time domain. Figure. 5 shows the flow diagram of the *I/Q* quadrature demodulation algorithm.

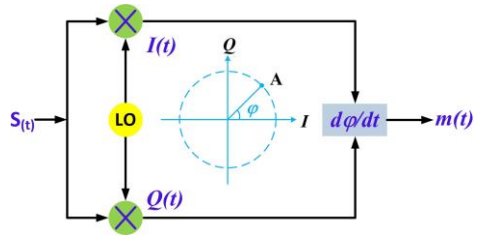

Fig. 4 Flow diagram of the arc-tangent demodulation algorithm

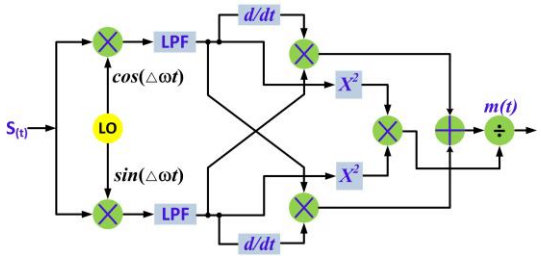

Fig. 5 Flow diagram of the improved I/Q quadrature demodulation algorithm

B. *Local carrier*

The kernel of the improved *I/Q* demodulation algorithm is mixing the frequency-modulated signal with two local carriers. The two local carriers have the same frequency with the beating signal. In practical applications, environmental perturbations, such as temperature, can cause drift of the polarization beat frequency. Therefore, it is impossible for us to keep the frequency of two local carriers strictly equal to the beat frequency. Assuming the frequency deviation of the local carrier with the beat frequency is $\delta\omega$. Then Eqs. (20) to (23) can be rewritten as

$$I(t) = \frac{1}{2}a(t)\cos\left[K_F\int m(t)\,dt - \delta\omega t + \Delta\varphi\right] \quad (25)$$

$$Q(t) = \frac{1}{2}a(t)\sin\left[K_F\int m(t)\,dt - \delta\omega t + \Delta\varphi\right] \quad (26)$$

$$I'(t) = \frac{1}{2}\left\{a'(t)\cos\left[K_F\int m(t)\,dt - \delta\omega t + \Delta\varphi\right] - a(t)\left[K_F m(t) - \delta\omega\right]\sin\left[K_F\int m(t)\,dt - \delta\omega t + \Delta\varphi\right]\right\} \quad (27)$$

$$Q'(t) = \frac{1}{2}\left\{a'(t)\sin\left[K_F\int m(t)\,dt - \delta\omega t + \Delta\varphi\right] + a(t)\left[K_F m(t) - \delta\omega\right]\cos\left[K_F\int m(t)\,dt - \delta\omega t + \Delta\varphi\right]\right\} \quad (28)$$

Then we can get

$$\frac{I(t)Q'(t) - I'(t)Q(t)}{I^2(t) + Q^2(t)} = K_F m(t) - \delta\omega = M(t) - \delta\omega \quad (29)$$

Therefore, we can get $M(t)$ by filtering the DC component $\delta\omega$. The improved *I/Q* demodulation algorithm can overcome the effect of the frequency drift of the local carrier.

IV. Experimental Results and Discussions

The experimental setup is shown in Fig. 6. The DFB fibre laser is 45 mm long and inscribed in Corning LVMX-1 erbium doped fibre using a 244 nm argon-ion laser. It was pumped by a 980 nm laser diode through a 980/1550 nm wavelength division multiplexer (WDM). An optical isolator was placed at the laser output to eliminate unwanted reflections. A polarizer and a polarization controller were used to maximize the beat signal. The laser output was injected into a high speed (3 GHz) photodetector (LBR-10M3G-10-15-10) and the beat signal was detected by an electrical spectrum analyzer or a demodulation system, which consists of a high-speed acquisition card and a PC.

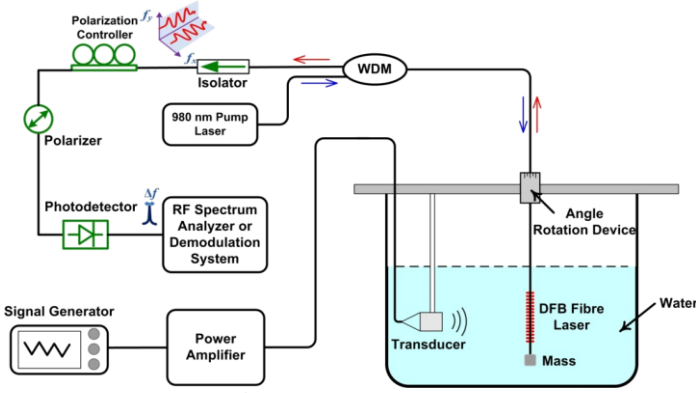

Fig. 6 Schematic diagram of the experimental setup.

In the experiments, the DFB fibre laser ultrasonic sensor was positioned in the far field of the ultrasonic transducer in a water tank. The periodic voltage waveform, which is supplied by an arbitrary signal generator and amplified by a power amplifier, was used to drive different plane ultrasonic transducers to generate ultrasound in the water. A mass was clamped at the end of the DFB fibre laser to keep the fibre straight.

A. Beat signal

In the first step, the high-speed photodetector was connected to a high-speed acquisition card. Figure. 7 shows the beat signal spectra of the DFB fibre laser, with no ultrasonic excitation, at different driving currents of the 980 nm pump laser. The frequency of the beat signal is about 182 MHz, and drift in the beat frequency due to environmental perturbations was observed. Unlike previous reports using DBR fibre lasers in Refs [7], [21]-[23], a pair of sidebands can be observed near the beat frequency.

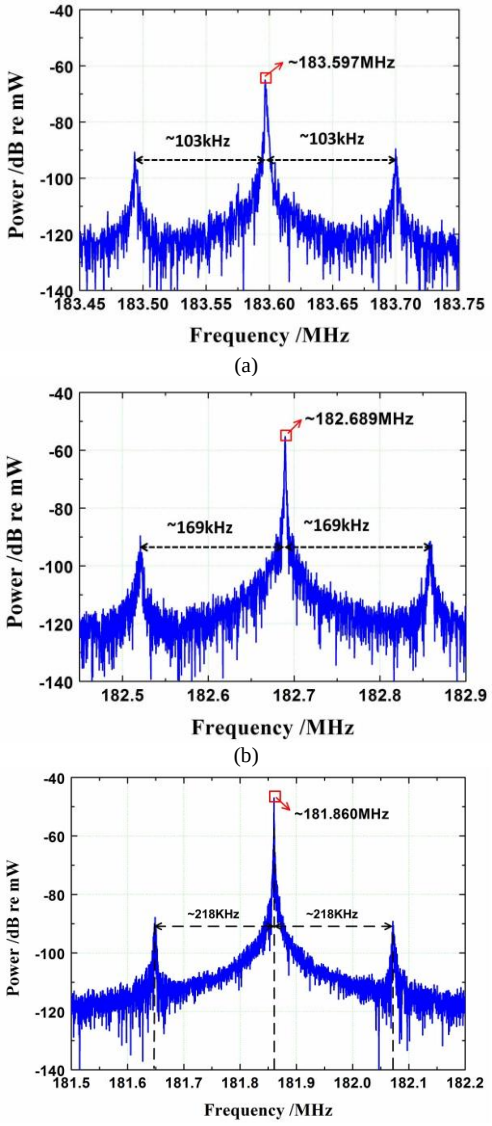

Fig. 7 Beat signal spectra of the DFB fibre laser at different driving currents of the 980nm pump laser. (a) 50 mA. (b) 100 mA. (c) 150 mA.

To confirm the modulation sidebands are due to the relaxation oscillation intensity noise [25], the laser pump power was increased and the frequency difference of the sidebands to the beat frequency showed a direct correlation with the relaxation oscillation RIN peak. The RIN of the DFB fibre laser with different driving currents was measured and shown in Fig. 8. The relaxation oscillation frequencies of the DFB fibre laser were 103 kHz, 169 kHz and 218 kHz under driving currents of 50 mA, 100 mA and 150 mA (corresponding to pump powers of 16 mW, 40 mW and 64 mW, respectively). The measurement results agree well with those in Fig. 7. It is interesting to note that the relaxation oscillation induced sidebands have not been reported in polarimetric sensors based on DBR lasers to the best of our knowledge. Whereas this is a potential limitation of the DFB laser structure; however, the

RIN relaxation oscillation noise peak can be reduced by increasing the grating coupling coefficient [2] or by applying electronic feedback to the pump laser [17].

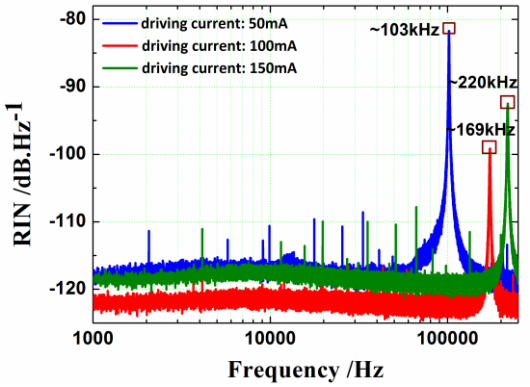

Fig. 8 The relative intensity noise of the DFB fibre laser at different driving currents of the 980 nm pump laser.

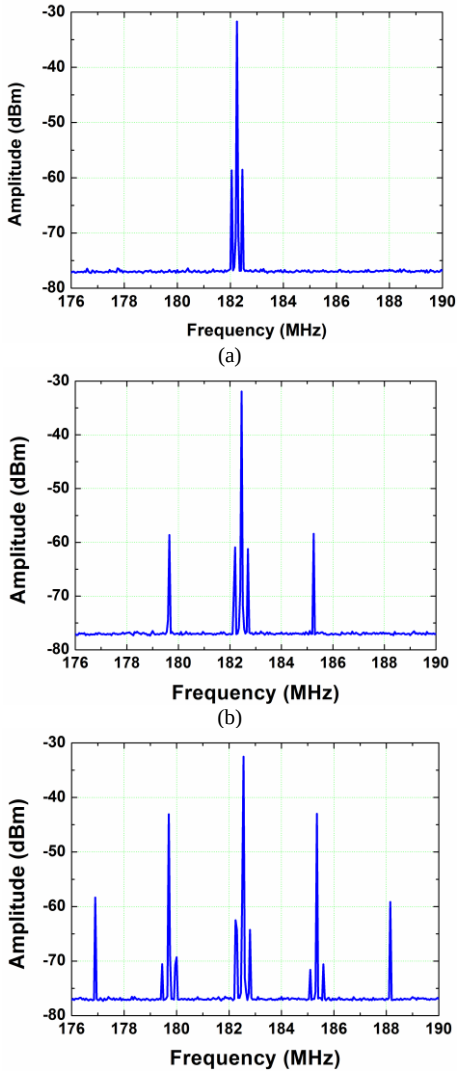

Fig. 9 Beat signal spectra of the DFB fibre laser as the acoustic transducer was driven with 2.25 MHz continuous signal at different voltages. (a) No driving voltage. (b) 2.3 V driving voltage. (c) 18.4 V driving voltage.

B. *Continuous ultrasonic signal*

A plane ultrasonic transducer with center frequency of 2.25 MHz was driven in continuous mode. The high-speed photodetector was connected to an electrical spectrum analyzer.

Figure. 9 shows the beat signal spectrum recorded by the spectrum analyzer when the ultrasonic transducer was driven at 2.25 MHz with different driving voltages. As expected, the beat signal was frequency modulated by the ultrasonic signal and sidebands appeared when the DFB fibre laser was subjected to the ultrasound signal; the sideband signal increased with the amplitude of the ultrasound. From Fig. 9, one can also find that the sidebands induced by the intensity noise (relaxation oscillation noise) of the DFB fibre laser always existed near the beat frequency, and also appeared near the ultrasonic sideband signal with increasing driving voltage. This phenomenon can be explained by Eqs. (13), (15) and (16).

C. *Ultrasonic Signals Demodulation*

To get the real-time waveforms of the ultrasonic signals, the beat signal was injected into a high-speed photodetector and recorded by using a high-speed acquisition card. Then, the ultrasonic signal was demodulated in software. The frequency and amplitude of the local carrier was 182 MHz and 1, respectively. Two 8th order low-pass digital Butterworth filter with cut-off frequency of 50 MHz were used to filter out the second-order beat frequency. The low frequency signal below 10 kHz of the demodulated signal was filtered by using a 5th order high pass digital filter.

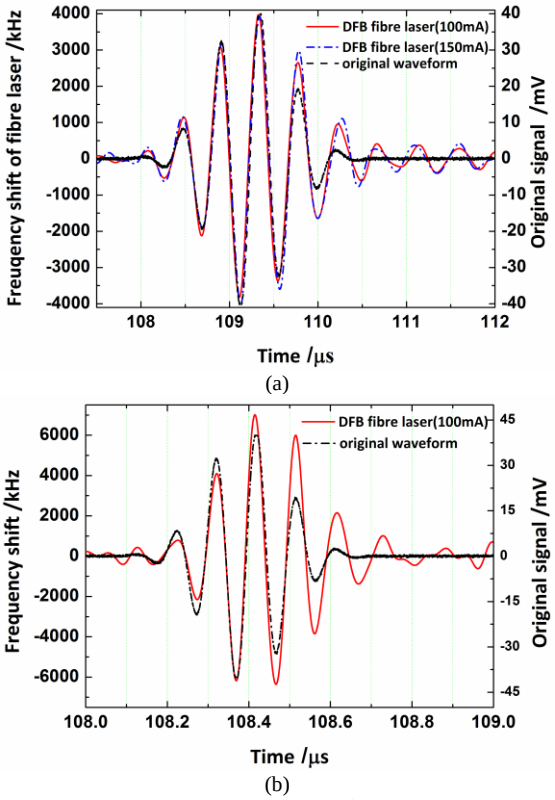

Fig. 10 Six-cycle burst signal detected by DFB fibre laser ultrasonic sensor comparing with original waveform generated by signal generator at different frequencies. (a) 2.25 MHz. (b) 10 MHz.

Six-cycle burst signals at frequencies of 2.25 MHz and 10 MHz, and a continuous harmonic signal at frequency of 2.25 MHz were used to drive different transducers to generate ultrasound in the water.

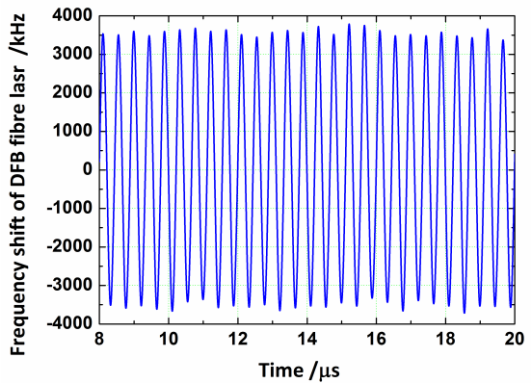

(a)

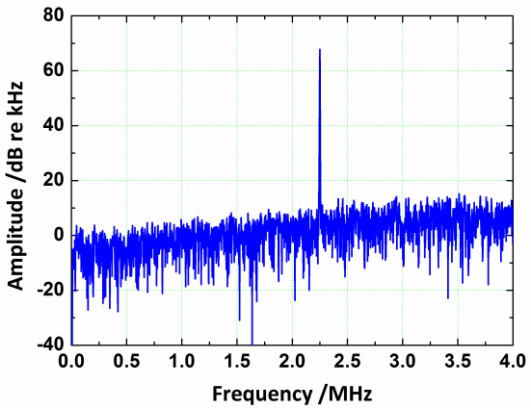

(b)

Fig. 11 Continuous harmonic signal detected by DFB fibre laser ultrasonic sensor. (a) Time domain. (b) Frequency domain.

Figure. 10 shows the output signals of the DFB fibre laser ultrasonic sensor (red line - pump current laser of 100 mA, blue dash line - pump laser current of 150 mA) at 2.25 MHz and 10 MHz. The original waveforms (black dash line) of the signal generator output, which are monitored by an oscilloscope, are superimposed for comparison. It should be noted that, the time axis of original waveforms in Fig. 10 has been shifted in order to get a better comparison with the output waveforms detected by the DFB fibre laser sensor. The exact starting time of the original waveforms is zero. The magnitudes of the measured responses at 2.25 MHz and 10 MHz vary due to the optical fibre's frequency response to ultrasound [14]. The detected ultrasonic waveform is in good agreement with the original input waveform, but shows some oscillations in tail position possibly due to the effect of the fibre coating. It is clear that, the DFB fibre laser sensor provides ideal waveform of ultrasound with high signal quality, and the improved I/Q quadrature demodulation method can demodulate the ultrasonic signal with high fidelity. Figure. 10(a) also shows the demodulated signals when the fibre laser was under different pump driving currents. This measurement result shows that the improved I/Q demodulation algorithm is robust against changes of pump power and corresponding changes of laser intensity.

Figure. 11 shows the continuous harmonic signal and the corresponding spectrum detected by DFB fibre laser ultrasonic sensor. From the experimental results, one can find that the improved I/Q demodulation algorithm can effectively eliminate the intensity noise of the fibre laser.

V. Conclusion

In this paper, the influences of the DFB fibre laser intensity noise on the polarimetric DFB fibre laser ultrasonic sensor have been studied systematically. The theoretical analysis predicts that the intensity noise of the DFB fibre laser and the ultrasonic signal will both induce sidebands in the beat signal of the DFB ultrasonic sensor. In comparison to previously reported work using DBR lasers, we show that with increasing amplitude of the ultrasonic signal, sidebands induced by the relaxation oscillation intensity noise also appear centered around the ultrasonic signal sidebands. The experimental results are in good accordance with theoretical analysis. In most cases, the beat signal of the DFB fibre laser can be treated as a small FM modulated signal, and the first order sidebands follow an approximate linear relationship with the applied ultrasonic signal in amplitude. In addition, a novel demodulation algorithm of the DFB fibre ultrasonic sensor is also investigated. The improved demodulation approach eliminates the effect of intensity noise on the DFB fibre laser and is robust against frequency drift of the local carrier.

References

[1] G. A. Cranch, G. M. H. Flockhart, and C. K. Kirkendall, "Distributed feedback fiber laser strain sensors," *IEEE Sensors J.*, vol. 8, no. 7-8, pp. 1161-1172, Jul-Aug 2008.

[2] S. B. Foster, G. A. Cranch, J. Harrison, A. E. Tikhomirov, and G. A. Miller, "Distributed Feedback Fiber Laser Strain Sensor Technology," *J. Lightw. Technol.*, vol. 35, no. 16, pp. 3514-3530, Aug 2017.

[3] G. A. Ball, G. Meltz, and W. W. Morey, "Polarimetric Heterodyning Bragg-Grating Fiber-Laser Sensor," *Opt. Lett.*, vol. 18, no. 22, pp. 1976-1978, Nov 1993.

[4] J. T. Kringlebotn, W. H. Loh, and R. I. Laming, "Polarimetric Er3+-doped fiber distributed-feedback laser sensor for differential pressure and force measurements," *Opt. Lett.*, vol. 21, no. 22, pp. 1869-1871, Nov 1996.

[5] L. Dong, W. H. Loh, J. E. Caplen, J. D. Minelly, K. Hsu, and L. Reekie, "Efficient single-frequency fiber lasers with novel photosensitive Er/Yb optical fibers," *Opt. Lett.*, vol. 22, no. 10, pp. 694–696, 1997.

[6] B. O. Guan, L. Jin, Y. Zhang, and H. Y. Tam, "Polarimetric heterodyning fiber grating laser sensors." *J. Lightw. Technol.*, vol. 30, no. 8. pp. 1097-1112, Apr. 2012.

[7] B. O. Guan, H. Y. Tam, S. T. Lau, and H. L. W. Chan, "Ultrasonic hydrophone based on distributed Bragg reflector fiber laser," *IEEE Photon. Technol. Lett.*, vol. 17, no. 1, pp. 169–171, Jan. 2005.

[8] L. Y. Shao, S. T. Lau, X. Dong, A. P. Zhang, H. L. W. Chan, H. Y. Tam, and S. He, "High-frequency ultrasonic hydrophone based on a cladding-etched DBR fiber laser," *IEEE Photon. Technol. Lett.*, vol.20, no. 8, pp. 548–550, Apr. 2008.

[9] S. T. Lau, L. Y. Shao, H. L. W. Chan, H. Y. Tam, C. H. Hu, H. H. Kim, R. Liu,Q. Zhou, and K.K. Shung, "Characterization of a 40-MHz focused transducer with a fiber grating laser hydrophone," *IEEE Trans. Ultrason., Ferroelectr., Freq. Control*, vol. 55, no. 12, pp. 2714–2718,Dec. 2009.

[10] T. Guo, A. C. L. Wong, W. Liu, B. O. Guan, C. Lu, and H. Y. Tam, "Beat-frequency adjustable Er-doped DBR fiber laser for ultrasound detection," *Opt. Exp.*, vol. 19, no. 3, pp. 2485–2492, 2011.

[11] D. Liu, Y. Liang, L. Jin, H. Sun, L. Cheng, and B. O. Guan, "Highly sensitive fiber laser ultrasound hydrophones for sensing and imaging applications." *Opt. Lett.*, vol. 41, no. 19, pp. 4530-4533, Oct. 2016.

[12] Y. Liang, L. Jin, L. Wang, X. Bai, L. Cheng and B. O. Guan, "Fiber-laser-based ultrasound sensor for photoacoustic imaging," *Sci. Rep.*, 7, 40849, Jan. 2017.
[13] B. O. Guan, L. Jin, L. Cheng, and Y. Liang, "Acoustic and Ultrasonic Detection with Radio-Frequency Encoded Fiber Laser Sensors," *IEEE J. Sel. Top. Quantum Electron.*, vol. 23, no. 2, pp. 302–313, 2017.
[14] R. P. Depaula, L. Flax, J. H. Cole, and J. A. Bucaro, "Single-Mode Fiber Ultrasonic Sensor," *IEEE J. Quantum Electron.*, vol. 18, no. 4, pp. 680-683, 1982.
[15] E. Rønnekleiv, "Frequency and Intensity Noise of Single Frequency Fiber Bragg Grating Lasers," *Opt. Fiber Technol.*, vol. 7, no. 3, pp. 206–235, 2001.
[16] G. A. Cranch, M. A. Englund, and C. K. Kirkendall, "Intensity noise characteristics of erbium-doped distributed-feedback fiber lasers," *IEEE J. Quantum Electron.*, vol. 39, no. 12, pp. 1579–1586, Dec. 2003.
[17] G. A. Cranch, "Frequency noise reduction in erbium-doped fiber distributed-feedback lasers by electronic feedback.," *Opt. Lett.*, vol. 27, no. 13, pp. 1114–6, Jul. 2002.
[18] S. Foster, A. Tikhomirov, and M. Milnes, "Fundamental thermal noise in distributed feedback fiber lasers," *IEEE J. Quantum Electron.*, vol. 43, no. 5-6, pp. 378-384, May-Jun 2007.
[19] S. Foster, G. A. Cranch, and A. Tikhomirov, "Experimental evidence for the thermal origin of 1/f frequency noise in erbium-doped fiber lasers," *Phys. Rev. A*, vol. 79, no. 5, Art no. 053802, May 2009.
[20] A. C. L. Wong, W. H. Chung, H. Y. Tam, and C. Lu, "Ultra-short distributed feedback fiber laser with sub-kilohertz linewidth for sensing applications," *Laser Physics*, vol. 21, no. 1, pp. 163-168, Jan 2011
[21] A. C. L. Wong *et al.*, "Extremely short distributed Bragg reflector fibre lasers with sub-kilohertz linewidth and ultra-low polarization beat frequency for sensing applications," *Meas. Sci. Technol.*, vol. 22, no. 4, p. 045202, Apr. 2011.
[22] J. H. Wo *et al.*, "Twist sensor based on axial strain insensitive distributed Bragg reflector fiber laser," *Opt. Express*, vol. 20, no. 3, pp. 2844-2850, Jan 2012.
[23] W. Liu, T. Guo, A. C. Wong, H.-Y. Tam, and S. He, "Highly sensitive bending sensor based on Er^{3+}-doped DBR fiber laser," *Opt. Express*, vol. 18, no. 17, p. 17834, Aug. 2010.
[24] H. L. W. Chan, K. S. Chiang, D. C. Price, and J. L. Gardner, "The characterization of high-frequency ultrasonic fields using a polarimetric optical fiber sensor," *J. Appl. Phys.*, vol. 66, pp. 1565 – 1570, 1989.
[25] H. Chen, Y. D. Tan, S. L. Zhang, and L. Q. Sun, "Study on mechanism of amplitude fluctuation of dual-frequency beat in microchip Nd:YAG laser," *Journal of Optics*, vol. 19, no. 1, Art no. 015702, Jan 2017.
[26] J. Canning, "Fibre lasers and related technologies," *Opt. Lasers Eng.*, vol. 44, no. 7, pp. 647–676, 2006.
[27] E. Rønnekleiv, M. Ibsen, M. N. Zervas, and R. I. Laming, "Characterization of intensity distribution in symmetric and asymmetric fiber DFB lasers," in *Conference on Lasers and Electro-Optics*, Vol. 6 of 1998 OSA Technical Digest Series Optical Society of America, Washington, D.C., p. 80, 1998.